# The fracture energy of ruptures driven by flash heating

Nicolas Brantut,[1] and Robert C. Viesca[2]

N. Brantut, Rock and Ice Physics Laboratory, Department of Earth Science, University College London, Gower Street, London WC1E 6BT, UK. (n.brantut@ucl.ac.uk)

Robert C. Viesca, Department of Civil and Environmental Engineering, Tufts University, 207A Anderson Hall, 200 College Avenue, Medford, MA 02155, USA. (robert.viesca@tufts.edu)

[1]Rock and Ice Physics and Seismological Laboratory, Department of Earth Sciences, University College London, London, UK.

[2]Department of Civil and Environmental Engineering, Tufts University, Medford, MA, USA.

We present a model for dynamic weakening of faults based on local flash heating at microscopic asperity contacts coupled to bulk heating at macroscopic scale. We estimate the fracture energy $G$ associated with that rheology, and find that for constant slip rate histories $G$ scales with slip $\delta$ as $G \propto \delta^2$ at small slip, while $G \propto \delta^{1/2}$ at large slip. This prediction is quantitatively consistent with data from laboratory experiments conducted on dry rocks at constant slip rate. We also estimate $G$ for crack-like ruptures propagating at constant speed, and find that $G \propto \delta^{2/3}$ in the large -slip limit. Quantiative estimates of $G$ in that regime tend to be several orders of magnitude lower than seismologically inferred values of $G$. We conclude that while flash heating provides a consistent explanation for the observed dynamic weakening in laboratory experiments with kinematically imposed slip, its contribution to the energy dissipation during earthquakes becomes negligible for large events when considerning the elastodynamic coupling between strength and slip evolution.

## 1. Introduction

The dynamics of earthquakes is primarily controlled by the balance between the available elastic strain energy (i.e., the pre-rupture stress level along the fault), the energy radiated away from the fault, and the fracture energy $G$ consumed to advance the rupture front. The fracture energy, far from being a material constant, depends on how the fault weakens during slip, and hence is ultimately controlled by the physical processes responsible for fault weakening.

In the context of seismology and shear rupture propagation with complex friction laws, $G$ is generally defined by the integral of the shear strength change over the local slip [e.g. *Kanamori and Heaton*, 2000; *Abercrombie and Rice*, 2005]. Therefore, $G$ integrates potentially complex strength evolution with slip, slip rate, and other evolving physical variables. Far-field seismological observations provide constraints on the magnitude of $G$, which is typically derived from estimates of moment magnitude and radiated energy [e.g. *Abercrombie and Rice*, 2005; *Viesca and Garagash*, 2015]. However, disentangling the details of stress, slip or slip rate evolution from $G$, is generally not possible (or at least not unequivocally) with seismological data alone [e.g. *Guatteri and Spudich*, 2000]. Hence, the physical mechanisms giving rise to earthquake propagation remain only accessible through a single integrated quantity, the fracture energy.

One approach to circumvent this issue and identify the underlying physics of dynamic weakening is to make predictions of $G$ based either on empirical laboratory data [*Nielsen et al.*, 2016] or theoretical analysis [*Rice*, 2006; *Viesca and Garagash*, 2015], and examine if and how the resulting scaling of $G$ with other source parameters (typically, fault

slip) matches with independent seismological estimates. In other words, the key question is: what does the observed scaling of $G$ tell us about the physics of rupture ? Such an approach has been remarkably successful in identifying thermal pressurisation as a potentially ubiquitous weakening mechanism, compatible with earthquake data over a very wide range of magnitudes [*Rice*, 2006; *Viesca and Garagash*, 2015]. Thermal pressurisation is a mechanism by which faults weaken due to an increase in pore fluid pressure on the fault plane driven by frictional heating. In a purely empirical approach, *Nielsen et al.* [2016] have shown that the fracture energy derived from laboratory friction experiments, almost regardless of the experimental conditions, is in fact consistent with that of earthquakes. These experimental results highlight the potential nonuniqueness of the weakening mechanisms responsible for the scaling of $G$ with slip: indeed, most of the experimental data used by *Nielsen et al.* [2016] were obtained on dry rocks, in a setup that essentially precludes the efficiency of thermal pressurisation.

Overall, a key question is to determine what features of weakening mechanisms are essential to reproduce the scaling of $G$ derived from seismological or experimental data, and whether weakening mechanisms other than thermal pressurisation could also be viable candidates to explain the fracture energy of earthquakes.

Here, we tackle this issue by exploring in detail the fracture energy associated with weakening by flash heating, which is a theoretically and experimentally documented weakening mechanism occurring at the onset of seismic slip [e.g. *Rice*, 1999, 2006; *Beeler et al.*, 2008; *Goldsby and Tullis*, 2011; *Passelègue et al.*, 2016; *Brantut et al.*, 2016]. We first present an updated flash heating model, which includes progressive weakening due to bulk frictional

heating, and then compute the associated fracture energy under either imposed slip rate or within an elastodynamic crack model. We then discuss the resulting scaling of $G$ with slip, and compare it to experimental and earthquake data. Finally, we extract several general conclusions about how fracture energy should scale with slip for ruptures driven by thermal weakening processes.

## 2. Flash heating model

### 2.1. Governing equations

The constitutive law governing frictional weakening by flash heating has been derived in detail by *Rice* [2006] and *Beeler et al.* [2008]. Here we develop a model for flash heating that is modified from the original formulation: following the steps initially outlined by *Rempel* [2006], and further developed by *Brantut and Platt* [2017] [see also *Proctor et al.*, 2014; *Yao et al.*, 2015], we include here the dependence of flash heating on the fault bulk temperature. We first recall the general form of the shear strength evolution governed by flash heating [*Rice*, 1999, 2006; *Beeler et al.*, 2008]:

$$\tau = \tau_0 \frac{V_\mathrm{w}(T)}{V}, \tag{1}$$

where $\tau$ is the strength, $\tau_0$ is the initial frictional strength of the fault, $V_\mathrm{w}$ is a critical weakening slip rate (temperature-dependent), and $V$ is the slip rate. Here we do not include any "residual" strength level, and assume that the strength at high slip rate approaches zero.

The weakening slip rate is given by[*Rice*, 2006]:

$$V_\mathrm{w}(T) = \frac{\pi\alpha}{D}\left(\frac{\rho c (T_\mathrm{w} - T)}{\tau_\mathrm{c}}\right)^2, \tag{2}$$

where $\alpha$ is the thermal diffusivity of the fault rock, $\rho c$ is its heat capacity , $D$ is the asperity contact diameter, $\tau_c$ is the asperity contact shear strength, and $T_w$ is the critical weakening temperature.

The evolution of the shear strength of the fault is given by the evolution of both the slip rate $V$ and fault zone temperature $T$. The latter is governed by the heat equation:

$$\frac{\partial T}{\partial t} = \alpha \frac{\partial^2 T}{\partial y^2} + \frac{\tau \dot{\gamma}}{\rho c}, \tag{3}$$

where $y$ is the spatial coordinate normal to the fault surface, and $\dot{\gamma}$ is the distributed shear strain rate in the fault gouge. For a gaussian strain rate distribution across the fault, Equation 3 has the following solution for temperaature evolution at $y = 0$ [*Carslaw and Jaeger*, 1959]:

$$T(t, y = 0) = T_0 + \frac{1}{\rho c} \int_0^t \frac{\tau(t')V(t')}{\sqrt{2\pi(w^2 + 2\alpha(t - t'))}} dt', \tag{4}$$

where $w$ is a measure of the shear zone thickness. Using the expression (1) for shear stress, we obtain an expression for temperature that does not include any direct dependence on slip rate:

$$T(t, y = 0) = T_0 + \frac{\tau_0}{\rho c} \int_0^t \frac{V_w[T(t')]}{\sqrt{2\pi(w^2 + 2\alpha(t - t'))}} dt'. \tag{5}$$

In our assumption of distributed strain rate over a finite thickness (and not bare surface contact), we implicitly extend the flash heating model to an ensemble of frictional contacts distributed over the fault thickness. This generalisation has been developed by *Rempel* [2006] and *Brantut and Platt* [2017], who showed that the model would hold provided that $V_w$ is modified by a factor proportional to the number of contacts within the fault thickness.

### 2.2. Solutions

In order to estimate the evolution of shear stress, and therefore of fracture energy, as a function of cumulated slip, one needs to solve Equation 5. Three informative end-member solutions can be found analytically.

At early times, while the fault effective thickness $w\sqrt{2\pi}$ remains large compared to the thermal boundary layer width $\sqrt{\alpha t}$, heating is mostly adiabatic and Equation (5) simplifies to:

$$T - T_0 \approx \frac{\tau_0}{\rho c w\sqrt{2\pi}} \int_0^t V_{\mathrm{w}}[T(t'))dt'. \tag{6}$$

Combining with expression (2) for the weakening velocity, we obtain the following solution for temperature:

$$T(t) = T_0 + (T_{\mathrm{w}} - T_0)\frac{t}{t + t_{\mathrm{w}}^{\mathrm{A}}}, \tag{7}$$

where

$$t_{\mathrm{w}}^{\mathrm{A}} = \frac{\rho c(T_{\mathrm{w}} - T_0)}{\tau_0}\frac{\sqrt{2\pi}w}{V_{\mathrm{w0}}} \tag{8}$$

with $V_{\mathrm{w0}} = V_{\mathrm{w}}(T_0)$. The time $t_{\mathrm{w}}^{\mathrm{A}}$ corresponds to the time required to heat a layer of thickness $\sqrt{2\pi}w$ from $T = T_0$ up to the weakening temperature $T_{\mathrm{w}}$. Equation (7) depends only on time and is not affected the slip rate history on the fault.

At large times, when the thermal boundary layer becomes much wider than the shear zone thickness, shear heating is essentially concentrated on an infinitely narrow width, which acts a line source. Under those conditions, Equation (5) simplifies to:

$$T - T_0 = \frac{\tau_0}{\rho c}\int_0^t \frac{V_{\mathrm{w}}[T(t')]}{\sqrt{4\pi\alpha(t - t')}}dt'. \tag{9}$$

A natural characteristic time in this regime is the following:

$$t_{\rm w}^{SP} = \alpha \left( \frac{\rho c (T_{\rm w} - T_0)}{\tau_0 V_{\rm w0}} \right)^2 , \tag{10}$$

which corresponds to the diffusion timescale that balances the nominal heat flux and the dissipation rate on the fault plane. A useful asymptotic solution, valid for $t \gg t_{\rm w}^{\rm SP}$, is given by (see Supplementary Materials, Section 1)

$$T(t) \approx T_0 + (T_{\rm w} - T_0)\sqrt{2} \left( \pi t / t_{\rm w}^{\rm SP} \right)^{-1/4} . \tag{11}$$

If we want to insist that the whole flash heating process occurs in the slip-on-a-plane limit, which is relevant for instance for bare rock frictional surfaces or when the two time scales $t_{\rm w}^{\rm A}$ and $t_{\rm w}^{\rm SP}$ are very different, we can also determine a simple asymptotic form for $T(t)$ in the small time limit. For $t_{\rm w}^{\rm A} \ll t \ll t_{\rm w}^{\rm SP}$, we find (see Supplementary Materials, Section 1) that the temperature is well approximated by

$$T(t) \approx T_0 + (1/2)(T_{\rm w} - T_0) \left( 1 - \exp(t/t_{\rm w}^{\rm SP}) \mathrm{erfc}(\sqrt{t/t_{\rm w}^{\rm SP}}) \right) . \tag{12}$$

Overall, for shear over a finite thickness, we observe that the temperature, and hence the strength evolution, is controlled by only two characteristic timescales, and therefore by only one nondimensional parameter, namely $t_{\rm w}^{\rm A}/t_{\rm w}^{\rm SP}$. This ratio of timescales controls the dominant thermal regime of the fault zone.

A set of numerical solutions of the general problem, computed using the spectral in space, finite-difference in time method given by *Noda and Lapusta* [2010], are shown in Figure 1(a) for a range of ratios $t_{\rm w}^{\rm A}/t_{\rm w}^{\rm SP}$, along with the asymptotic solution derived above. The corresponding evolution of strength, computed using (1) and $V = V_{\rm w0}$, is given in

Figure 1(b). We observe a gradual decrease in strength over time, due to the reduction in $V_w(T)$ induced by the macroscopic heating of the fault.

## 3. Fracture energy

Based on our strength computations, we can now make predictions for the fracture energy associated with flash heating. Here we use the generalised definition of $G$ given by *Abercrombie and Rice* [2005]:

$$G(\delta) = \int_0^\delta (\tau[\delta'] - \tau[\delta]) d\delta', \tag{13}$$

where $\delta$ is the slip. Since the strength depends directly on the slip rate history, we also expect the fracture energy to do so. In the following, we analyse how $G$ scales with slip using two models for slip rate evolution, one with constant slip rate, and one derived from elastodynamics.

### 3.1. Analysis using constant slip rate

In a first approximation, we use a simple assumption of constant slip rate to compute $G$. In this case, analytical formulae can be derived for $G(\delta)$ in the three asymptotic cases outlined in the previous Section. In the adiabatic regime, a direct computation of (13) using $\delta = Vt$ yields:

$$G(\delta) = \rho c (T_w - T_0) w \sqrt{2\pi} \left( \frac{\delta}{V t_w^A + \delta} \right)^2 \quad \text{(adiabatic)}. \tag{14}$$

In the slip-on-a-plane approximation, in the small slip limit (i.e., $Vt_w^A \ll \delta \ll Vt_w^{SP}$), an approximate form for the fracture energy is (see Supplementary Materials, Section 2)

$$G(\delta) \approx \tau_0 \delta_w^{SP} \times \frac{2}{3\sqrt{\pi}} \left( \frac{\delta}{\delta_w^{SP}} \right)^{3/2} \quad \text{(slip on a plane, small slip)}, \tag{15}$$

where $\delta_{\rm w}^{\rm SP} = V_{\rm w0} t_{\rm w}^{\rm SP}$. Finally, a slip-on-a-plane, large slip approximation is given by (see Supplementary Materials, Section 2):

$$G(\delta) \approx \tau_0 \delta_{\rm w}^{\rm SP} \times \frac{2}{\sqrt{\pi}} \left( \frac{\delta}{\delta_{\rm w}^{\rm SP}} \right)^{1/2} \quad \text{(slip on a plane, large slip)}, \tag{16}$$

which is valid for $\delta \gg V t_{\rm w}^{\rm SP}$.

The results for $G(\delta)$ in the general case (computed numerically) and the approximate analytical solutions are shown in Figure 2. Essentially, we find that there is a switch from $G \propto \delta^2$ at small slip to $G \propto \sqrt{\delta}$ at large slip; if the two timescales $t_{\rm w}^{\rm A}$ and $t_{\rm w}^{\rm SP}$ are separated, an intermediate regime arises where $G \propto \delta^{3/2}$. This behaviour is completely analogous to the scaling given by *Rice* [2006] for weakening by thermal pressurisation.

The reason for the similarity between flash heating and thermal pressurisation in this context is the fact that, at small slip, both mechanisms are essentially similar to linear slip-weakening; whereas at large slip, both mechanisms are dominated by a thermal weakening mechanisms controlled by a thermal (and/or hydraulic) diffusive boundary layer.

### 3.2. Analysis using a dynamic crack model

The kinematic approach outlined above gives initial insight into the scaling of fracture energy with slip. However, using a constant slip rate is a simplification, inconsistent with the mechanics of rupture propagation in which slip rate evolves in concert with strength behind the rupture tip.

For a semi-inifinite shear crack propagating at constant speed, the elastodynamic equilibrium requires that

$$\tau(x) = \frac{\mu^*}{2\pi V_{\rm r}} \int_0^\infty \frac{V(s)}{s-x} ds, \tag{17}$$

where $x$ is the position from the rupture tip, $V_\mathrm{r}$ is the rupture speed and $\mu*$ is an elastic shear modulus which depends on the mode of rupture and on the rupture speed [*Rice*, 1980]. The elastodynamic stress (17) has to be consistent with the strength on the fault given by the flash heating process (Equation 1). Therefore, the slip rate, stress and temperature histories are coupled and have to be determined simultaneously.

Far from the crack tip, for large slip, an asymptotic analysis of the coupled system (17), (1) and (9) (see Supplementary Materials, Section 2) leads to the following approximation for the fracture energy:

$$G(\delta) \approx \tau_0 \delta_\mathrm{w}^\mathrm{SP} \left( \frac{\mu^* V_\mathrm{w0}}{3\pi\tau_0 V_\mathrm{r}} \right)^{1/3} \left( \frac{\delta}{\delta_\mathrm{w}^\mathrm{SP}} \right)^{2/3} . \tag{18}$$

Notably, $G$ scaling with a 2/3-power law in slip was also found by *Viesca and Garagash* [2015] for dynamic ruptures driven by thermal pressurisation.

## 4. Comparison with Laboratory and Earthquake Data

The theoretical results outlined in the previous Section can be compared to laboratory data obtained at high constant (imposed) slip rate. Figure 3 shows the fracture energy compilation of *Nielsen et al.* [2016] as a function slip, plotted together with the theoretical predictions for flash heating using a realistic set of parameter values [*Brantut and Platt*, 2017]: constant slip rate $V = 1$ m/s, critical time $t_\mathrm{w}^\mathrm{SP} = 0.1$ s, critical slip rate $V_\mathrm{w0} = 0.2$ m/s, and nominal stress $\tau_0 = 20$ MPa. The flash heating model reproduces the shift in trend, modelled here as a transition between $\delta^{3/2}$ at small slip and $\delta^{1/2}$ at large slip.

The theoretical results for the dynamic crack-tip problem can be used to see whether we can also explain earthquake fracture energy data with flash heating only. This is attempted in Figure 4, which shows the $G$ vs. $\delta$ data compiled by *Viesca and Garagash*

[2015] together with the large slip asymptote obtained from the dynamic steady-state crack analysis. We used a rupture speed $V_r$ equal to around 90% of the shear wave speed, so that the elastodynamic shear modulus $\mu^*$ is reduced by approximately a factor 2 compared to its static value.

Even though the set of parameters used in the simulation are similar to that used to fit the laboratory data, the fracture energy predicted by the model remains much smaller than for earthquakes over a significant range of slip ($\delta > 10^{-2}$ m). Beyond 10 mm slip, the fracture energy from flash heating is much smaller than for earthquakes, implying that other dissipation processes dominate (e.g., thermal pressurisation). This is consistent with previous estimates for the relative contribution of flash heating vs. thermal pressurisation [*Brantut and Rice*, 2011]. At small slip distances, the earthquake data are consistent with a scaling of $G$ with $\delta^2$, as for instance produced by a linear slip-weakening friction law or by thermal pressurisation of pore fluids. Note that slip-weakening is not necessarily incompatible with the physics of flash heating, since there must be a critical slip distance beyond which asperities start to weaken at high speed [e.g. *Noda et al.*, 2009; *Brantut and Rice*, 2011; *Viesca and Garagash*, 2015]. Here, we did not include any slip-weakening process in our flash heating model in order to explore the properties of the thermal weakening process alone. It appears that the involvement of an element of slip weakening at small slip distances within the flash heating framework is necessary to produce a more realistic scaling of fracture energy with slip.

Despite the similarity in the scaling of $G$ with slip between thermal pressurisation and flash heating at large slip ($G \propto \delta^{2/3}$), any quantitative estimate using realistic parameter values reveals that flash heating has a negligible contribution in $G$.

## 5. Discussion and Conclusion

Laboratory data are explained quantitatively well by the flash heating model, but not earthquake data, especially for slip distances larger than a few millimetres. By contrast, *Viesca and Garagash* [2015] have shown that thermal pressurisation is able explain earthquake data over 9 orders of magnitude in slip. This difference is due mostly to the low heat diffusivity of rocks, which make critical weakening times and distances for flash heating very short compared to those linked with thermal pressurisation (see Supplementary Materials, Section 3). Indeed, the characteristic slip distance associated with thermal pressurisation is governed by the hydraulic diffusivity of fault rocks, which is widely variable and typically orders of magnitude larger than their thermal diffusivity. In addition, the large slip rates arising in the elastodynamic crack model tend to induce a faster strength reduction than in constant slip rate cases, therefore producing overall lower fracture energies.

Despite the quantitative discrepancies between flash heating and thermal pressurisation, for both processes the fracture energy at large slip scales with $\delta^{1/2}$ at constant slip rate and with $\delta^{2/3}$ for propagating ruptures. This similarity is not coincidental; in fact, *any* thermal weakening process for which temperature remains bounded at large times would produce similar scalings of $G$ with slip. Indeed, the large slip asymptote is obtained by observing that (1) $V(x)$ and $\tau(x)$ both decrease with same power $x^\lambda$ far from the crack

tip (Equation 17, see *Viesca and Garagash* [2015] and Supplementary Materials), and (2) the integral in (4) approaches a constant, finite temperature for sufficiently large times. These requirements imply that $\lambda = -1/4$, from which $G \propto \delta^{2/3}$ is deduced.

By contrast, the apparent stronger scaling of $G$ with $\delta^2$ at small slip merely reflects a linear slip-weakening process. Thermal pressurisation under adiabatic, undrained conditions is a likely possibility, but may not be the only one. For instance, a regularised flash heating process including an instrinsic critical slip distance for asperities to weaken [*Noda et al.*, 2009] would also be a possibility.

From a phenomenological point of view, brittle fracture of intact rocks is also characterised by a slip-weakening process [e.g. *Ohnaka*, 2003]; so does rate-and-state friction at moderate slip rates (i.e., in the absence of healing or state recovery). Any of these phenomena is compatible with seismological estimates of $G(\delta)$ for small slip (typically $\delta \lesssim 1$ cm).

In summary, the most general conclusion that can be drawn from the comparison of friction models and seismological constraints of fracture energy is that seismic slip occurs by a succession or combination of physical processes which (1) initially resemble linear slip-weakening, and (2) progressively become dominated by diffusion across the fault. In other words, the progressive change in scaling of $G$ vs. slip with increasing slip imply that shear work dissipation occurs more and more outside the fault, either due to thermal or hydraulic diffusion (as in flash heating or thermal pressurisation), or alternatively by off-fault damage (as explained by *Andrews* [1976, 2005]; *Nielsen et al.* [2016]).

The theoretical developments presented here show that great care is required when comparing friction models (empirical or physics-based) to earthquake data: except for the purely slip-dependent friction laws, boundary conditions in terms of slip rate history generally have an impact on the strength evolution and on the resulting fracture energy. Dynamic steady-state rupture models [e.g. *Garagash*, 2012; *Viesca and Garagash*, 2015] provide a useful tool to circumvent the shortcomings of assuming *a priori* slip rate histories, without having to resort to computationnally intensive numerical elastodynamic simulations.

**Acknowledgments.** This work was initiated following discussions with John D. Platt, whom both authors would like to gratefully acknowledge. NB received support from the UK Natural Environment Research Council through grant NE/K009656/1. RCV is grateful for support from NSF grant EAR-1344993 and from the Southern California Earthquake Center (SCEC). SCEC is funded by NSF Cooperative Agreement EAR-1033462 and USGS Cooperative Agreement G12AC20038. The SCEC contribution number for this paper xxx. The analytical formulae and numerical methods described in the main text and supplementary materials are sufficient to reproduce all the results presented in the paper.

## References

Abercrombie, R. E., and J. R. Rice, Can observations of earthquake scaling constrain slip weakening ?, *Geophys. J. Int.*, *162*, 406–424, 2005.

Andrews, D. J., Rupture propagation with finite stress in antiplane strain, *J. Geophys. Res.*, *81*(20), 3575–3582, 1976.

Andrews, D. J., Rupture dynamics with energy loss outside the slip zone, *J. Geophys. Res.*, *110*, B01307, doi:10.1029/2004JB003191, 2005.

Beeler, N. M., T. E. Tullis, and D. L. Goldsby, Constitutive relationships and physical basis of fault strength due to flash heating, *J. Geophys. Res.*, *113*, B01401, doi:10.1029/2007JB004988, 2008.

Brantut, N., and J. D. Platt, Dynamic weakening and the depth dependence of earthquake faulting, in *Fault Zone Dynamic Processes: Evolution of Fault Properties During Seismic Rupture*, *Geophys. Monogr. Ser.*, vol. 227, edited by M. Y. Thomas, T. M. Mitchell, and H. S. Bhat, American Geophysical Union, Washington, DC, (accepted), 2017.

Brantut, N., and J. R. Rice, How pore fluid pressurization influences crack tip processes during dynamic rupture, *Geophys. Res. Lett.*, *38*, L24314, doi:10.1029/2011GL050044, 2011.

Brantut, N., F. X. Passelègue, D. Deldicque, J.-N. Rouzaud, and A. Schubnel, Dynamic weakening and amorphization in serpentinite during laboratory earthquakes, *Geology*, *44*(8), 607–610, doi:10.1130/G37932.1, 2016.

Carslaw, H. S., and J. C. Jaeger, *Conduction of heat in solids*, 2nd ed., Oxford University Press, New York, 1959.

Garagash, D. I., Seismic and aseismic slip pulses driven by thermal pressurization of pore fluid, *J. Geophys. Res.*, *117*, B04314, doi:doi:10.1029/2011JB008889, 2012.

Goldsby, D. L., and T. E. Tullis, Flash heating leads to low frictional strength of crustal rocks at earthquake slip rates, *Science*, *334*, 216–218, 2011.

Guatteri, M., and P. Spudich, What can strong-motion data tell us about slip-weakening fault-friction laws ?, *Bull. Seism. Soc. Am.*, *90*(1), 98–116, 2000.

Kanamori, H., and T. H. Heaton, Microscopic and macroscopic physics of earthquakes, in *Geocomplexity and the Physics of Earthquakes*, *Geophys. Monogr. Ser.*, vol. 120, edited by J. B. Rundle, D. L. Turcotte, and W. Klein, American Geophysical Union, Washington, DC, 2000.

Nielsen, S., E. Spagnuolo, S. A. F. Smith, M. Violay, G. Di Toro, and A. Bistacchi, Scaling in natural and laboratory earthquakes, *Geophys. Res. Lett.*, *43*, 1504–1510, doi:10.1002/2015GL067490, 2016.

Noda, H., and N. Lapusta, Three-dimensional earthquake sequence simulations with evolving temperature and pore pressure due to shear heating: Effect of heterogeneous hydraulic diffusivity, *J. Geophys. Res.*, *115*, B12314, doi:10.1029/2010JB007780, 2010.

Noda, H., E. M. Dunham, and J. R. Rice, Earthquake ruptures with thermal weakening and the operation of major faults at low overall stress levels, *J. Geophys. Res.*, *114*, B07302, doi:10.1029/2008JB006143, 2009.

Ohnaka, M., A constitutive scaling law and a unified comprehension for frictional slip failure, shear fracture of intact rock, and earthquake rupture, *J. Geophys. Res.*, *108*(B2), 2080, doi:10.1029/2000JB000123, 2003.

Passelègue, F. X., A. Schubnel, S. Nielsen, H. S. Bhat, D. Deldicque, and R. Madariaga, Dynamic rupture processes inferred from laboratory microearthquakes, *J. Geophys.*

306 *Res.*, *121*, doi:10.1002/2015JB012694, 2016.

307 Proctor, B. P., T. M. Mitchell, G. Hirth, D. Goldsby, F. Zorzi, J. D. Platt, and G. Di
308 Toro, Dynamic weakening of serpentinite gouge and bare-surfaces at seismic slip rates,
309 *J. Geophys. Res.*, *119*, doi:10.1002/2014JB011057, 2014.

310 Rempel, A. W., The effects of flash-weakening and damage on the evolution of fault
311 strength and temperature, in *Earthquakes: radiated energy and the physics of faulting*,
312 *Geophys. Monogr. Ser.*, vol. 170, edited by R. Abercrombie, A. McGarr, G. Di Toro,
313 and H. Kanamori, pp. 263–270, American Geophysical Union, Washington, DC, 2006.

314 Rice, J. R., The mechanics of earthquake rupture, in *Physics of the Earth's Interior*,
315 edited by A. M. Dziewonski and E. Boschi, Proc. Intl. School of Physics E. Fermi,
316 Italian Physical Society/North Holland Publ. Co., 1980.

317 Rice, J. R., Flash heating at asperity contacts and rate-depend friction, *Eos. Trans. AGU*,
318 *80*(46), Fall Meet. Suppl., F6811, 1999.

319 Rice, J. R., Heating and weakening of faults during earthquake slip, *J. Geophys. Res.*,
320 *111*, B05311, doi:10.1029/2005JB004006, 2006.

321 Viesca, R. C., and D. I. Garagash, Ubiquitous weakening of faults due to thermal pres-
322 surization, *Nat. Geosci.*, doi:10.1038/ngeo2554, 2015.

323 Yao, L., S. Ma, J. D. Platt, A. Niemeijer, and T. Shimamoto, The crucial role of temper-
324 ature in high-velocity weakening of faults: Experiments on gouge using host blocks of
325 different thermal conductivities, *Geology*, doi:10.1130/G37310.1, 2015.

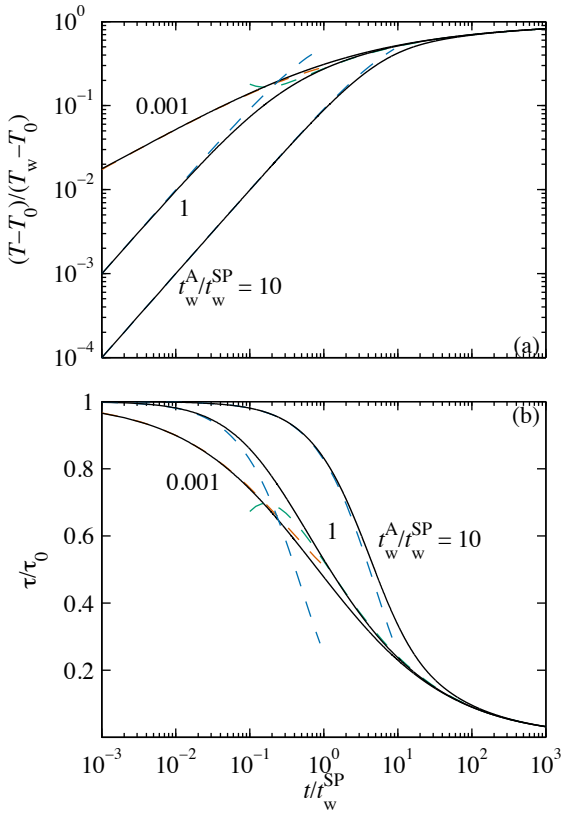


**Figure 1.** Evolution of temperature (a) and strength (b) with time during flash heating for a range of timescale ratios $t_w^A/t_w^{SP}$. The evolution of temperature (a) is independent from the slip rate history. In the computation of strength we assumed $V = V_{w0}$. The black curves correspond to the full numerical solution for each ratio of timescales. The dashed blue lines correspond to the asymptotic solutions in the adiabatic regime, the dashed green lines are the asymptotic solutions for the slip-on-a-plane regime in the large time limit, and the dashed orange lines are the asymptotic solution for the slip-on-a-plane regime in the small time limit.

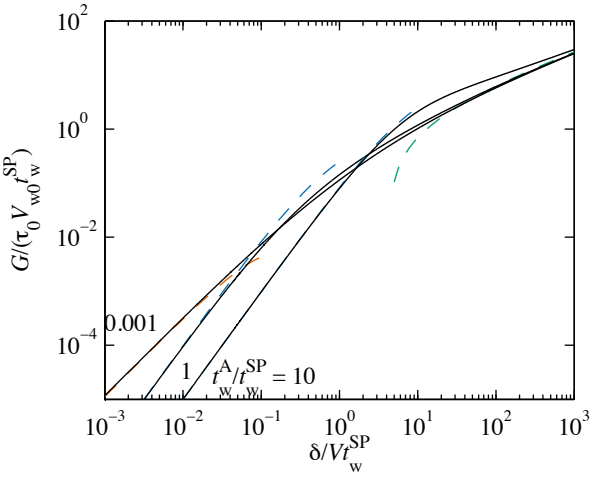


**Figure 2.** Evolution of fracture energy with slip during flash heating. This evolution is computed using a constant imposed slip rate. The black curves correspond to the full numerical solution for the given ratio of timescales $t_w^A/t_w^{SP}$. The dashed blue lines correspond to the asymptotic solution in the adiabatic regime, the dashed green line is the asymptotic solution for the slip-on-a-plane regime for large time, and the dashed orange line is the asymptotic solution for the slip-on-a-plane regime for small time.

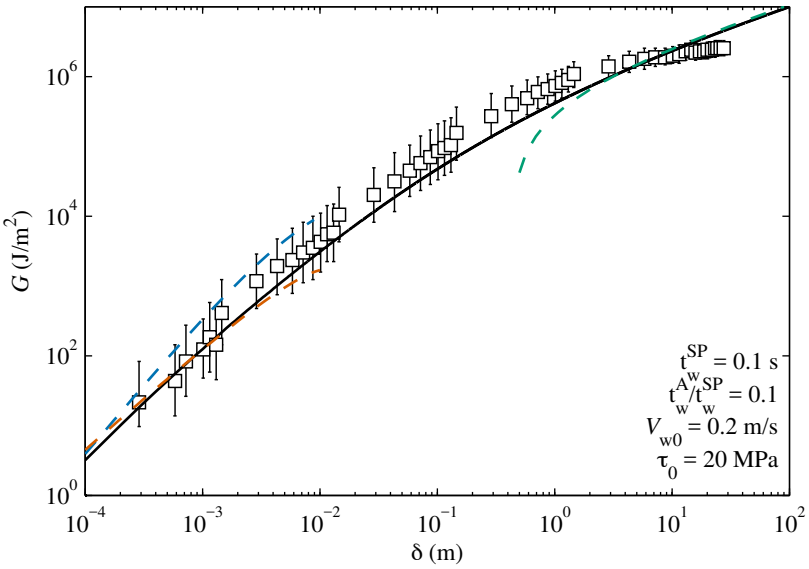


**Figure 3.** Comparison of laboratory-derived fracture energy from high speed friction experiments [*Nielsen et al.*, 2016] (squares) and theoretical predictions for flash heating. The general numerical solution is given by the solid black line, the large slip asymptote is the green dashed line, the small slip (adiabatic) asymptote is the blue dashed line, and the small slip (slip-on-a-plane) asymptote is the orange dashed line. Parameter values are listed in the graph.

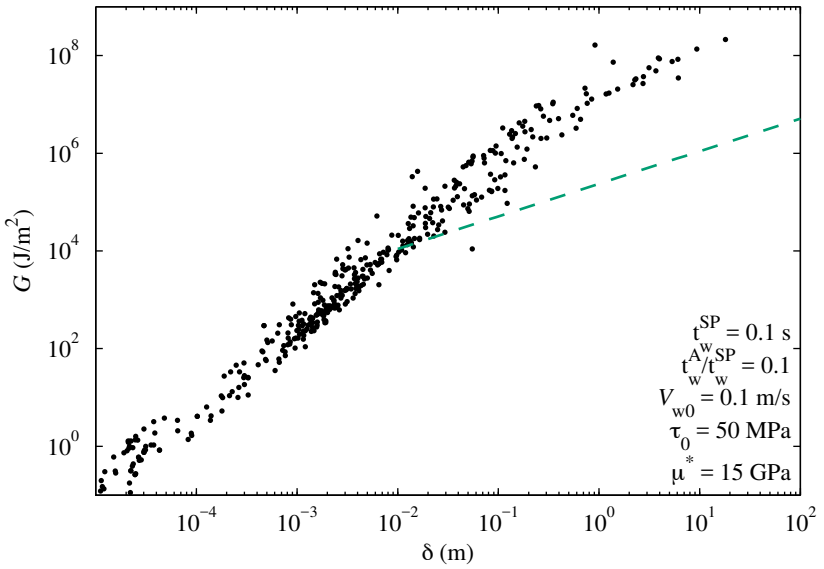


**Figure 4.** Comparison of earthquake fracture energy estimates (taken from the compilation of *Viesca and Garagash* [2015]) and the semi-infinite crack model driven by flash heating only (large slip asymptote shown as the green dashed line). Parameter values are reported in the graph.

# Supplementary Information for "The fracture energy of ruptures driven by flash heating"

Nicolas Brantut*and Robert C. Viesca†

May 10, 2017

## 1 Temperature asymptotics for the slip on a plane approximation

**Large times.** Introducing a nondimensional temperature rise $\theta = (T-T_0)/(T_\mathrm{w}-T_0)$ and a nondimensional time $u = t/t_\mathrm{w}^\mathrm{SP}$, Equation (9) of the main text is conveniently rewritten as

$$\theta(u) = \frac{1}{2\sqrt{\pi}} \int_0^u \frac{(1-\theta(u'))^2}{\sqrt{u-u'}} du'. \tag{1}$$

Unfortunately, we could not find an analytical solution to Equation (1) in the general case. However, we determined a useful asymptotic solution for large $u$ by looking for solutions of the form

$$\theta(u) = 1 - \epsilon(u) \tag{2}$$

with $\epsilon(u) \to 0$ as $u \to \infty$. Equation (1) is then rewritten as

$$1 - \epsilon(u) = \frac{1}{2\sqrt{\pi}} \int_0^u \frac{\epsilon(u')^2}{\sqrt{u-u'}} du'. \tag{3}$$

This can be solved approximately by looking for simple expressions for $\epsilon(u)$ which ensure that leading order terms on each side are balanced correctly. In a first approximation, we should find $\epsilon(u)$ so that the integral on the l.h.s. is of $O(1)$. By inspecting the integral on the l.h.s., we can see that $\epsilon(u) \propto u^{-1/4}$ will indeed integrate to a constant. Matching the leading order terms leads to the following asymptotic approximation for $\epsilon(u)$:

$$\epsilon(u) \approx \sqrt{2}(\pi u)^{-1/4}. \tag{4}$$

*Rock and Ice Physics and Seismological Laboratory, Department of Earth Sciences, University College London, London, UK.

†Department of Civil and Environmental Engineering, Tufts University, Medford, MA, USA.

A better approximation can be found by trying to match higher order terms, namely a term in $u^{-1/4}$ on the r.h.s. We then use $\epsilon(u) = au^{-1/4} + bu^{-1/2}$, compute the integral (discarding singular terms appearing only for small $u$, where our approximation is not relevant) and match the first two terms, which lead to the following approximation:

$$\epsilon(u) \approx \sqrt{2}(\pi u)^{-1/4} - \frac{\Gamma(3/4)}{\Gamma(1/4)} u^{-1/2}, \tag{5}$$

or simply $\epsilon(u) \approx (1.0623)u^{-1/4} - (0.3380)u^{-1/2}$.

**Early times.** In that case we look for solutions $\theta(u)$ of Equation (1) for small $u$. Linearising the integrand for small $u$ (and therefore for small $\theta(u)$), and integrating by parts, we find that

$$\theta(u) \approx \sqrt{u/\pi} - \frac{1}{\sqrt{\pi}} \int_0^u \frac{\theta(u')}{\sqrt{u-u'}} du'. \tag{6}$$

This is a linear Abel integral equation of the second kind for $\theta$, and can be solved straightforwardly, which yields:

$$\theta(u) \approx (1/2) \left(1 - \exp(u)\mathrm{erfc}(\sqrt{u})\right). \tag{7}$$

# 2 Fracture energy asymptotics in the slip on plane limit

Throughout this Section we use a normalised time $u = t/t_{\mathrm{w}}^{\mathrm{SP}}$, temperature $\theta = (T - T_0)/(T_{\mathrm{w}} - T_0)$, strength $\tilde{\tau} = \tau/\tau_0$ and slip rate $v = V/V_{\mathrm{w}0}$. The natural characteristic slip scale is therefore $\delta^* = V_{\mathrm{w}0} t_{\mathrm{w}}^{\mathrm{SP}}$, and the characteristic scale for fracture energy is $G^* = \tau_0 \delta^*$. With these notations, the constitutive law (Equation 1 in the main text) becomes:

$$\tilde{\tau} = (1 - \theta)^2 / v, \tag{8}$$

and the normalised fracture energy $\tilde{G} = G/G^*$ is

$$\tilde{G} = \int_0^{\delta'} (\tilde{\tau}[\delta] - \tilde{\tau}[\delta']) d\delta, \tag{9}$$

where $\delta' = \delta/\delta^*$ is the normalised slip.

At constant slip rate, (9) becomes

$$\tilde{G} = \int_0^u \left((1 - \theta(u'))^2 - (1 - \theta(u))^2\right) du'. \tag{10}$$

**Small slip, constant slip rate.** In the small slip limit, slip-on-a-plane regime, an approximate form of the fracture energy can be determined by expanding $\theta(u)$ for small $u$:

$$\theta(u) \approx \sqrt{u/\pi} - u/2, \tag{11}$$

and then use that approximation in the computation of $\tilde{G}$ in Equation 10. The result is then

$$\tilde{G} \approx \frac{2}{3\sqrt{\pi}} u^{3/2} - \frac{\pi+1}{2\pi} u^2. \tag{12}$$

Retaining only the leading order term, the dimensional form of (12) reads

$$G \approx G^* \frac{2}{3\sqrt{\pi}} (\delta'/v)^{3/2}, \tag{13}$$

which is the same as Equation (15) in the main text.

**Large slip, constant slip rate.** In a similar fashion, a large time approximation can be found based on the asymptotic approximation for $\theta(u)$ given in Equation (5). After direct integration of (10), we find:

$$\tilde{G} \approx 2\sqrt{\frac{u}{\pi}} - 6\sqrt{2}\frac{\Gamma(3/4)}{\Gamma(1/4)} \left(\frac{u}{\pi}\right)^{1/4}. \tag{14}$$

Again, retaining only the leading order term yields the following dimensional form for the fracture energy:

$$G \approx 2G^* \sqrt{\frac{\delta'}{\pi v}}, \tag{15}$$

which is the same as Equation (16) in the main text.

**Large slip, dynamic crack solution.** For a semi-inifinite shear crack propagating at constant speed, we recall that the elastodynamic equilibrium implies that

$$\tau(x) = \frac{\mu^*}{2\pi V_\mathrm{r}} \int_0^\infty \frac{V(s)}{s-x} ds, \tag{16}$$

where $x$ is the position from the rupture tip, $V_\mathrm{r}$ is the rupture speed and $\mu*$ is an elastic shear modulus modified according to the rupture speed (*Rice*, 1980). Normalising the position by $x^* = V_\mathrm{r} t_\mathrm{w}^\mathrm{SP}$, Equation 16 is rewritten as

$$\tilde{\tau}(u) = \frac{\mu'}{2\pi} \int_0^\infty \frac{v(u')}{u'-u} du', \tag{17}$$

where

$$\mu' = \frac{\mu^* V_\mathrm{w0}}{\tau_0 V_\mathrm{r}}. \tag{18}$$

Following *Viesca and Garagash* (2015), we look for asymptotic solutions of (17) in the form $v(u) = Bu^\lambda$ and $\tau(u) = -\mu'(B/2)\mathrm{cotan}(\pi\lambda)u^\lambda$ also satisfying

(asymptotically for large $u$) Equation (1) and the constitutive law (8). As observed in the previous Section, at large $u$, Equation (1) implies that $\theta \approx 1 - \sqrt{2}(\pi u)^{-1/4}$. The constitutive law (8) then implies that:

$$\tilde{\tau} v \approx 2/\sqrt{(}\pi u). \tag{19}$$

Using $v(u) = Bu^{\lambda}$ and $\tau(u) = -\mu'(B/2)\mathrm{cotan}(\pi\lambda)u^{\lambda}$ in (19) yields:

$$\lambda = -1/4 \qquad \text{and} \qquad B = 2/(\mu'^{1/2}\pi^{1/4}), \tag{20}$$

so that

$$v(u) \approx (2/\sqrt{\mu'})(\pi u)^{-1/4} \quad \text{and} \quad \tilde{\tau}(u) \approx \sqrt{\mu'}(\pi u)^{-1/4}. \tag{21}$$

The (normalised) slip distance is given by

$$\delta' = \int_0^u v(u')du', \tag{22}$$

from which we compute $u \approx [(3/8)\mu'^{1/2}\pi^{1/4}\delta']^{4/3}$. The stress as a function of slip is therefore given by

$$\tau(\delta') \approx \left(\frac{8\mu'}{3\pi}\right)^{1/3} \delta'^{-1/3}, \tag{23}$$

which can be integrated straightforwadly to yield

$$\tilde{G}(\delta') \approx \left(\frac{\mu'}{3\pi}\right)^{1/3} \delta'^{2/3}. \tag{24}$$

The dimensional form of (24) corresponds to Equation (18) of the main text.

# 3 Comparison of characteristic scales between flash heating and thermal pressurisation

In order to compare the weakening produced by flash heating and thermal pressurisation, it is instructive to compute the ratio $r_{\mathrm{FH/TP}}$ of the characteristic slip weakening distances associated with each process. In the adiabatic regime, the ratio is

$$r^{\mathrm{A}}_{\mathrm{FH/TP}} = \frac{t^{\mathrm{A}}_{\mathrm{w}} V}{\rho c \sqrt{2\pi} w/(f\Lambda)}, \tag{25}$$

where $\Lambda$ denotes the thermal pressurisation factor (*Rice*, 2006). Assuming that the friction coefficient $f$ relevant for thermal pressurisation is equal to the initial friction coefficient before flash heating operates, Equation 25 simplifies to

$$r_{\mathrm{FH/TP}} = \frac{T_{\mathrm{w}} - T_0}{T_{\mathrm{max}} - T_0} \frac{V}{V_{\mathrm{w0}}}, \quad \text{(adiabatic)} \tag{26}$$

where $T_{\max} = \sigma_0'/\Lambda$ is the maximum temperature rise associated with adiabatic, undrained thermal pressurisation ($\sigma_0'$ denotes the initial effective normal stress on the fault). For typical crustal parameter values (*Brantut and Platt*, 2017), $r_{\mathrm{FH/TP}}$ is of the order of 10, which implies that progressive weakening by adiabatic flash heating occurs over much larger slip distances than thermal pressurisation. We note, however, that flash heating has an "instantaneous" effect (occurring over distances of a few tens of microns) that will always occur first if $V$ is significantly greater than $V_{\mathrm{w0}}$ (*Brantut and Rice*, 2011). Thermal pressurisation therefore dominates the initial weakening only when $V \lesssim V_{\mathrm{w0}}$. This is the case only for relatively thick gouge layers, since $V_{\mathrm{w0}}$ increases proportionally to the number of contacts over which sliding occurs within the gouge.

In the slip-on-a-plane limit, the relevant slip scales for flash heating and thermal pressurisation are $t_{\mathrm{w}}^{\mathrm{SP}} V$ and $L^*$, respectively, where

$$L^* = \frac{4\alpha^*}{V}\left(\frac{\rho c}{f\Lambda}\right)^2. \tag{27}$$

In the expression for $L^*$, the diffusivity $\alpha^*$ is a combined hydraulic and thermal diffusivity (e.g. *Garagash*, 2012). In the limit of large hydraulic diffusivity compared to thermal diffusivity, which is most likely the case in nature, $\alpha^*$ is approximately equal to the hydraulic diffusivity itself. The ratio of characteristic slip distances for flash heating and thermal pressurisation is therefore

$$r_{\mathrm{FH/TP}} = \frac{\alpha}{\alpha^*}\left(\frac{T_{\mathrm{w}} - T_0}{T_{\max} - T_0}\frac{V}{V_{\mathrm{w0}}}\frac{f}{f_0}\right)^2, \quad \text{(slip-on-a-plane)} \tag{28}$$

where $f$ is the friction coefficient operating during thermal pressursation, and $f_0$ is the initial friction coefficient before flash heating occurs. The ratio $f/f_0$ is likely less than one, and more critically we generally have $\alpha/\alpha^* \ll 1$, so that the ratio $r_{\mathrm{FH/TP}}$ is much less than 1 for realistic crustal fault properties (see *Viesca and Garagash*, 2015; *Brantut and Platt*, 2017).

# References


Brantut, N., and J. D. Platt, Dynamic weakening and the depth dependence of earthquake faulting, in *Fault Zone Dynamic Processes: Evolution of Fault Properties During Seismic Rupture*, *Geophys. Monogr. Ser.*, vol. 227, edited by M. Y. Thomas, T. M. Mitchell, and H. S. Bhat, American Geophysical Union, Washington, DC, (accepted), 2017.

Brantut, N., and J. R. Rice, How pore fluid pressurization influences crack tip processes during dynamic rupture, *Geophys. Res. Lett.*, *38*, L24314, doi: 10.1029/2011GL050044, 2011.

Garagash, D. I., Seismic and aseismic slip pulses driven by thermal pressurization of pore fluid, *J. Geophys. Res.*, *117*, B04314, doi: doi:10.1029/2011JB008889, 2012.

Rice, J. R., The mechanics of earthquake rupture, in *Physics of the Earth's Interior*, edited by A. M. Dziewonski and E. Boschi, Proc. Intl. School of Physics E. Fermi, Italian Physical Society/North Holland Publ. Co., 1980.

Rice, J. R., Heating and weakening of faults during earthquake slip, *J. Geophys. Res.*, *111*, B05311, doi:10.1029/2005JB004006, 2006.

Viesca, R. C., and D. I. Garagash, Ubiquitous weakening of faults due to thermal pressurization, *Nat. Geosci.*, doi:10.1038/ngeo2554, 2015.